HHS Public Access

Author manuscript

Oncogene. Author manuscript; available in PMC 2021 December 14.

Published in final edited form as:

Oncogene. 2021 July ; 40(27): 4592–4603. doi:10.1038/s41388-021-01874-7.

Statins reduce castration-induced bone marrow adiposity and prostate cancer progression in bone

Tianhong Pan[1,*], **Song-Chang Lin**[2,*], **Yu-Chen Lee**[2,*], **Guoyu Yu**[2], **Jian H. Song**[3], **Jing Pan**[2], **Mark Titus**[3], **Robert L. Satcher**[1], **Theocharis Panaretakis**[3], **Christopher Logothetis**[3], **Li-Yuan Yu-Lee**[4], **Sue-Hwa Lin**[2,3,#]

[1]Department of Orthopedic Oncology, University of Texas, MD Anderson Cancer Center, Houston, TX, United States of America

[2]Department of Translational Molecular Pathology, University of Texas, MD Anderson Cancer Center, Houston, TX, United States of America

[3]Department of Genitourinary Medical Oncology, University of Texas, MD Anderson Cancer Center, Houston, TX, United States of America

[4]Department of Medicine, Baylor College of Medicine, Houston, Texas 77030, United States of America

Abstract

A fraction of patients undergoing androgen deprivation therapy (ADT) for advanced prostate cancer (PCa) will develop recurrent castrate-resistant PCa (CRPC) in bone. Strategies to prevent CRPC relapse in bone are lacking. Here we show that the cholesterol-lowering drugs statins decrease castration-induced bone marrow adiposity in the tumor microenvironment and reduce PCa progression in bone. Using primary bone marrow stromal cells (BMSC) and M2-10B4 cells, we showed that ADT increases bone marrow adiposity by enhancing BMSC-to-adipocyte transition *in vitro*. Knockdown of androgen receptor abrogated BMSC-to-adipocyte transition, suggesting an androgen receptor-dependent event. RNAseq analysis showed that androgens reduce the secretion of adipocyte hormones/cytokines including leptin during BMSC-to-adipocyte transition. Treatment of PCa C4-2b, C4-2B4 and PC3 cells with leptin led to an increase in cell cycle progression and nuclear Stat3. RNAseq analysis also showed that androgens inhibit cholesterol biosynthesis pathway, raising the possibility that inhibiting cholesterol biosynthesis may decrease BMSC-to-adipocyte transition. Indeed, statins decreased BMSC-to-adipocyte transition *in vitro* and castration-induced bone marrow adiposity *in vivo*. Statin pre-treatment

[#]Corresponding author: Sue-Hwa Lin, Department of Translational Molecular Pathology, Unit 89, The University of Texas MD Anderson Cancer Center, 1515 Holcombe Blvd., Houston, TX 77030. Phone: 713-794-1559; Fax: 713-834-6084; slin@mdanderson.org.

[*]These authors contributed equally to this work

Conflict of interest disclosure:

C. J. Logothetis reports receiving commercial research grants from Bayer, Sanofi, Janssen, Astellas Pharma, Pfizer; and honoraria from Bayer, Janssen, Sanofi, Astellas Pharma. No potential conflicts of interest are disclosed by the other authors.

Data deposition: The RNASeq data has been deposited. The GEO accession number is “GSE174516”.

reduced 22RV1 PCa progression in bone after ADT. Our findings with statin may provide one of the mechanisms to the clinical correlations that statin use in patients undergoing ADT seems to delay progression to “lethal” PCa.

Keywords

bone marrow stromal cells; adipocytes; statin; prostate cancer; bone metastasis; androgen depletion

Introduction

Androgen-deprivation therapy (ADT) is the standard treatment for patients with high risk prostate cancer (PCa) [1]. However, a fraction of these patients will develop castrate-resistant PCa (CRPC), which frequently occurs in bone [2]. The striking predilection of PCa to progress in bone suggests that the bone microenvironment plays a central role in disease progression. Metastatic PCa in bone is the lethal progression of the disease and is difficult to treat [3]. So far, there is no established strategies to prevent or delay PCa progression in bone. Delineating bone microenvironment components that are involved in the development of CRPC in bone may lead to strategies to prevent or delay PCa progression in bone.

Recently, several clinical correlative studies found that the use of the cholesterol-lowering drug statin seems to have a beneficial effect in preventing or delaying bone metastasis in patients undergoing androgen-depletion therapy (ADT). Platz et al. [4] analyzed data from a prospective cohort study of 34,989 US male health professionals and found that statin use was associated with a reduced risk of advanced PCa, especially metastatic or fatal, but not with overall risk of PCa. In the international retrospective observational STABEN study that included patients receiving abiraterone or enzalutamide for metastatic CRPC, statin use was significantly associated with both prolonged overall survival and cancer-specific survival, and increased >30% early PSA declines [5]. In another study that examined an ADT cohort of 926 patients, it was found that men taking statins had a longer median time-to-progression during ADT compared with nonusers [6]. These clinical observations raise the intriguing possibility that statins may have an effect on preventing or delaying PCa relapse in bone. However, due to inconsistent clinical observations [7], statin use for bone metastasis prevention has not been recommended.

We and others have shown that PCa cells in bone are in close communication with the bone microenvironment that supports cancer cell survival, proliferation and resistance to chemotherapy [8, 9]. The mechanisms by which bone marrow microenvironment supports CRPC growth in bone are not completely understood. Bone marrow is comprised of a variety of cells, including hematopoietic stem cells, adipocytes, osteoclasts, osteoblasts, and immune cells. Some cells, e.g., bone marrow stromal cells, can be induced to differentiate into various cell lineages when triggered by different environmental conditions [10]. One of the major cell types in bone marrow are adipocytes. Adipocytes in prostate tumor microenvironment have been shown to promote PCa progression [11]. Studies have demonstrated that high fat diet leads to an increase in bone marrow adipocytes that support

PCa progression in bone [12], suggesting that bone marrow adipocytes play a role in PCa progression in bone.

While ADT is effective in inhibiting PCa growth, ADT also leads to many changes in the bone microenvironment. One side effect of long-term ADT is the loss of bone density that leads to an increase in fractures [13]. A better understanding of the mechanisms that lead to PCa relapse in bone after ADT could identify strategies for preventing bone metastasis. Here, we examined the effect of ADT on bone marrow stromal cell (BMSC)-to-adipocyte transition and found that cholesterol synthesis pathways are involved in this process. We further showed that the cholesterol biosynthesis inhibitor statin reduces BMSC-to-adipocyte transition and castration-induced bone marrow adiposity, and that statin treatment delays PCa progression in bone.

Results

Androgen depletion enhances BMSC-to-adipocyte transition

We examined androgen-depletion therapy (ADT)-induced changes in bone marrow using castration. Male CD1 mice (22-week-old) were castrated and histological analysis of the femurs was performed 6 weeks post-castration. H&E staining (Fig. 1A, left) and bone histomorphometry analysis (Fig. 1A, middle) showed that there were more adipocytes in the bone marrow of femurs from castrated mice compared to control mice. Quantification of the number of adipocytes per area showed a significant increase in adipocyte density from 3.81 ± 1.73 in intact mice to 21.89 ± 8.39 per mm^2 after castration (Fig. 1A, right). We isolated bone marrow cells from femurs of mice with or without castration. qRT-PCR of the RNAs from these cells showed that the expression of adipocyte markers, including adiponectin (Adipoq), perilipin (Plin) and nuclear receptor peroxisome proliferator-activated receptor-γ (PPARγ), were all significantly increased in bone marrow cells prepared from castrated mice relative to intact normal mice (Fig. 1B). These observations suggest that castration has an effect on bone microenvironment by increasing the density of adipocytes.

Bone marrow stromal cell (BMSC) have been shown to be able to become adipocytes through BMSC-to-adipocyte transition [14, 15]. Castration-mediated increases in bone marrow adiposity may be through a direct effect of androgens on BMSC-to-adipocyte transition or indirectly through other castration-induced events. We isolated BMSCs from femurs of CD1 mice (6-week-old), cultured them in medium containing charcoal-stripped serum (CSS) for 7 days, followed by treatment with androgens DHT or R1881 in adipocyte differentiation medium (ADM) for an additional 5 days. Under this ADM condition, BMSCs differentiated into adipocytes that contained a large amount of lipid droplets in the cytoplasm, as determined by Oil red-O (ORO) staining, whereas significantly less ORO-positive cells were observed after DHT (10 nM) or R1881(10 nM) treatment (Fig. 1C). The reduction in adipocytes were also determined by counting the number of ORO-positive cells and by quantification of ORO extract (Fig. 1C, left). Similarly, culturing M2-10B4 cells, a BMSC-derived cell line [16], in ADM with DHT or R1881 resulted in the inhibition of adipocyte formation compared to its non-treated control (Fig. 1C, right). Inhibition of adipogenic differentiation by DHT or R1881 was confirmed by qRT-PCR, which showed that expression of adipocyte-related genes *Adipoq*, *Plin*, *Fabp4* and lipoprotein lipase (*Lpl*)

were also significantly reduced by DHT or R1881 in both BMSC and M2-10B4 cells (Fig. 1D). These results suggest that androgens have a direct effect in suppressing BMSC-to-adipocyte transition.

Androgen receptor mediates the suppression of BMSC-to-adipocyte transition by DHT

As androgens have genomic and non-genomic effects [17], we examined whether androgen receptor (AR) plays a role in DHT-mediated inhibition of BMSC-to-adipocyte transition. *Ar* gene expression was transiently knocked down in M2-10B4 cells by *Ar* siRNAs. Both AR protein (Fig. 2A) and *Ar* mRNA (Fig. 2B) levels were reduced in *Ar* knockdown clones M2-10B4-#73si*Ar*, M2-10B4-#75si*Ar* and M2-10B4-#79si*Ar* when compared with M2-10B4-NS non-silencing control. Forty-eight hours after siRNA transfection, cells were cultured in ADM with or without DHT for an additional 5 days. We found that DHT-mediated inhibition of adipocyte formation was partially abrogated in all three *Ar* knockdown clones, as determined by ORO staining, counting ORO-positive cells and quantification by ORO extraction (Fig. 2C). Similar results were observed when AR was knocked down in BMSCs isolated from bone marrow of CD1 mouse femurs (Fig. 2D). These results suggest that DHT-mediates inhibition of BMSC-to-adipocytes transition through AR (Fig. 2E).

RNAseq analysis of androgen-mediated events during BMSC-to-adipocyte transition

We used RNAseq to examine androgen-mediated events during BMSC-to-adipocyte transition. We found that when M2-10B4 cells were cultured in ADM, 1542 genes were up-regulated and 102 canonical pathways were markedly (z score > 2) and significantly ($p < 0.05$) up-regulated as compared to control. The top 10 up-regulated pathways include adipogenesis-related pathways, such as fatty acid beta-oxidation, oxidative phosphorylation, TCA cycle II, and amino acid degradation (Fig. 3A, left), suggesting an increase in fatty acid synthesis accompanied with an inhibition of protein synthesis. The top 10 up-regulated genes include those that are related to fatty acid oxidation and fatty metabolism such as *Adipoq*, *Cidec*, *Fabp4*, *Cyp2e1*, *Cd36*, and *Plin1* (Fig. 3A), consistent with the activation of adipogenesis program. We found that 94 pathways and 1628 genes were significantly down-regulated when M2-10B4 cells were induced in ADM as compared to control. The top 10 down-regulated pathways during adipogenesis include EIF2 signaling, kinetochore metaphase signaling pathway, and cell cycle control of chromosomal replication (Fig. 3B, left), suggesting an inhibition of cell cycle progression during adipocyte differentiation. The top 10 down-regulated genes include *Tnmd,* which is a marker for tendon and ligament lineage cells and its deletion in tendon stem/progenitor cells accelerates adipogenic differentiation accompanied with increased *Pparγ* and *Lpl* mRNA levels [18], and *BMP4*, which stimulates osteoblast differentiation, osteoblast mineralization, bone mineralization and bone growth (Fig. 3B, right). These results suggest a coordinated up-regulation of adipogenesis-related genes and inhibition of cell cycle progression during BMSC-to-adipocyte transition.

Androgen-mediated events are represented by genes whose expression is up-regulated during adipogenesis but down-regulated by DHT treatment and, conversely, genes whose expression is down-regulated during adipogenesis but up-regulated by DHT. We found

that when BMSC cells were treated with DHT during adipogenesis (ADMDHT), 610 genes were down-regulated by DHT (Fig. 3C, left). Amongst these DHT down-regulated genes are 463 genes that are found to be up-regulated during adipogenesis (ADM vs control). The cellular distribution of these 463 commonly regulated genes is shown (Fig. 3C, right). Fig. 3D shows the top 10 DHT down-regulated pathways and the top 10 DHT down-regulated genes during BMSC-to-adipocyte transition. Consistent with the inhibition of adipogenesis by DHT, adipogenesis-related pathways such as fatty acid beta-oxidation, oxidative phosphorylation and TCA cycle II were down-regulated by DHT treatment (Fig. 3D). Interestingly, we observed that the cholesterol biosynthesis pathway is inhibited by DHT (Fig. 3D, red arrow), and the most DHT down-regulated gene, Ephx2, is a gene whose mutations are associated with familial hypercholesterolemia [19]. These observations suggest that inhibitors of cholesterol biosynthesis may be used to overcome ADT-mediated BMSC-to-adipocyte transition.

Adipocyte-secreted factors including leptin stimulate prostate cancer cell cycle progression and cell proliferation

As secreted factors may have effects on cells in the adjacent environment, we analyzed adipocyte-secreted factors whose expression was inhibited by DHT. RNAseq analysis showed that 32 genes belong to this group. Three growth factors including *Lep*, *Nrg4*, *Vegfb* and three cytokines including *GPr151*, *Cxcl13*, *Il1rn* were significantly increased in ADM (vs control) and decreased in ADMDHT (vs ADM) as indicated by FPKM values shown in the heatmap (Fig. 4A). The fold changes in the expression of these 6 adipocyte-secreted factors in response to various culture conditions are shown (Fig. 4B). We found that with ADM treatment, the levels of *leptin*, *Nrg4* and *Cxcl13* were increased by 3.3-, 2.1- and 1.6-fold, respectively. We further confirmed the up-regulation of leptin, Nrg4 and Cxcl13 in adipogenesis (ADM) condition and their down-regulation by DHT (ADMDHT) by qRT-PCR analysis (Fig. 4C). Protein levels of leptin in the conditioned medium from the four experimental groups were further confirmed using ELISA (Fig. 4D). These results indicate that androgen-mediated inhibition of adipocyte formation also reduces the release of growth factors and cytokines from adipocytes into the bone marrow microenvironment.

We next examined whether conditioned medium from bone marrow adipocytes (Adipo-CM) affects the growth of PCa cells. We generated C4-2B4-FUCCI (fluorescent ubiquitination-based cell cycle indicator) cells [20], which stably co-express a G1 phase reporter (red fluorescence) and an S-G2M phase reporter (green fluorescence) (Fig. 4E, left). Briefly, the G1 and S-G2M reporters are regulated by cell cycle-dependent E3 ubiquitin ligase activities that oscillate over the cell cycle to label nuclei red during G1 and green during S-G2M. Using live-cell imaging, we monitored the dynamic shift of C4-2B4-FUCCI cells from G1 (red) into S-G2M (green) at the single cell level (Fig. 4E, right). We found that in the presence of Adipo-CM, the percentage of C4-2B4-FUCCI cells entering S-G2M was significantly increased as compared to media control (Fig. 4F, left). Given that leptin was highly expressed during BMSC-to-adipocyte transition (Fig. 4D), we further tested the effect of leptin on PCa cell cycle progression. We found that the percentage of C4-2B4-FUCCI cells entering S-G2M was significantly higher in leptin-treated cells than in control cells (Fig. 4F, right), indicating that leptin stimulates PCa cell cycle progression from G1 into

S phase. We found that leptin also significantly increased the proliferation of C4-2b and PC3 cells by Presto blue assay and cell counting (Fig. 4G). It was reported that leptin induces growth of cancer cells via activation of Stat3 [21]. We found an increase in Stat3 translocation into the nucleus of C4-2B4 cells treated with Adipo-CM (Fig. 4H) or leptin (Fig. 4I) as compared to their controls, suggesting that leptin mediates PCa cell proliferation through Stat3 activation. Taken together, our studies suggest that androgen depletion enhances BMSC-to-adipocyte transition, leading to an increase in adipocyte-secreted factors, some of which stimulate PCa cell proliferation (Fig. 4J).

Statins suppress BMSC-to-adipocyte transition *in vitro*

We considered whether strategies that reduce BMSC-to-adipocyte transition may delay or prevent PCa progression in bone. Our RNAseq analysis showed that cholesterol biosynthesis pathway was inhibited by DHT (Fig. 3D). Thus, we examined whether statins, the cholesterol biosynthesis inhibitors [22, 23], can be used to inhibit BMSC-to-adipocyte transition. BMSC or M2-10B4 cells were cultured in ADM to stimulate BMSC-to-adipocyte transition with or without statins. We found that both atorvastatin and rosuvastatin reduced adipocyte formation, as determined by ORO-positive cell numbers and ORO extraction, by about 50% in BMSC (Fig. 5A) and M2-10B4 cells (Fig. 5B) relative to non-treated controls. qRT-PCR analysis showed that transcript levels of adipocyte markers, including *Adipoq, Plin, Fabp4, Lpl and Pparγ,* were significantly decreased by atorvastatin and rosuvastatin treatment (Fig. 5C). Similar suppressive effects on adipocyte formation were also observed with additional statins, including fluvastatin, lovastatin, mevastatin and simvastatin (Supplementary Fig. S1). Furthermore, atorvastatin and rosuvastatin caused a significant decrease in transcript and protein levels of leptin (Fig. 5D). These observations suggest that statins can inhibit BMSC-to-adipocyte transition *in vitro* (Fig. 5E).

Statins reduce BMSC-to-adipocyte transition *in vivo*

We further examined the effect of statins on castration-induced bone marrow adiposity *in vivo*. Male CD1 mice (12-week-old) were administered orally with atorvastatin (10 mg/kg/day) or vehicle once a day for one week followed by castration or sham-operation. Atorvastatin treatment was continued for an additional 6 weeks (Fig. 6A) and femurs were collected for analyses. Bone histomorphometry analysis showed that castration caused a significant increase in adipocyte numbers (Ad N/TV or Ad N/BV), which were reduced with atorvastatin treatment (Fig. 6B). Castration also caused an increase in osteolysis, as reflected in an increase in bone surface covered with osteoclasts (OC.S/BS), surface eroded by osteoclasts (ES/BS) and eroded surface with osteoclasts (ES(OC+)/BS) (Fig. 6C). Such increases were not reversed by atorvastatin treatment (Fig. 6C). Castration seemed to cause a slight change in the levels of osteoblasts, as reflected in Ob.S/BS and N.Ob/B.Pm.; however, other osteoblast-related parameters, including OS(Ob+)/BS and N.Ob/T.Ar, did not reach significance with castration, nor did atorvastatin treatment further affect these parameters (Fig. 6D). Overall, castration led to decreases in bone volume (BV/TV), bone surface density (BS/TV) and trabecular bone density (Tb. N), and an increase in trabecular separation (Tb. Sp) (Fig. 6E). Although there was a slight trend towards reversal of such decreases by atorvastatin, no statistical significance was reached (Fig. 6E). We further conducted micro-CT scans of femurs (Fig. 6F). Analysis of trabecular area showed that

castration caused a decrease in trabecular bone mineral density (Tb. BMD), trabecular bone volume (Tb. BV/TV), trabecular bone surface density (Tb. BS/TV), and trabecular bone thickness (Tb. Th), and such decreases were either not significantly or only marginally reversed by atorvastatin (Fig. 6F), findings that are similar to those measured by bone histomorphometry (Fig. 6E). These results indicate that atorvastatin treatment can reduce castration/ADT-mediated increase in adipocytes, but not osteoclasts or other bone-related parameters.

Stain pre-treatment reduces prostate cancer progression in bone after androgen depletion therapy

Our studies showed that castration generates a bone microenvironment enriched with adipocytes, which secrete growth factors/cytokines, e.g. leptin, which may enhance PCa progression in bone. Because we also showed that statins can reduce adiposity from castration, we examined whether statin pre-treatment can reduce PCa progression in bone after androgen depletion therapy. SCID mice (20-week-old) were orally administered with atorvastatin or vehicle for 10 days before castration and throughout the duration of the study. Mice were then castrated to generate an adipocyte-enriched bone microenvironment. Two weeks after castration, mice were inoculated with luciferase-Tomato labeled 22RV1 cells (22RV1/LT) by intracardiac injection to allow PCa cells to disseminate to bone (Fig. 6G). Metastasis of 22RV1/LT cells to bone was monitored by bioluminescence imaging. However, because the disseminated cells were too low to be detected by bioluminescence imaging at four-weeks post tumor cell inoculation, qPCR for human *Alu* repetitive sequences was used to quantify the number of tumor cells in mouse femurs. *Alu* qPCR showed that 22RV1 cells have disseminated to and proliferated in the femurs of both control and atorvastatin-treated mice (Fig. 6H, left). However, atorvastatin treatment significantly reduced the number of 22RV1 PCa cells in femur (Fig. 6H, right). These observations suggest that statin pre-treatment can reduce PCa progression in bone after androgen depletion therapy.

Discussion

We have shown that androgen depletion increases bone marrow adiposity through BMSC-to-adipocyte transition and statins partially reverse such an event (Fig. 6I). Adipocytes have long been considered to play a role in enhancing PCa growth in primary site [11, 24–27]. Podgorski's group [12, 28] further showed that high fat diet enhances the development of metastatic PCa in bone. We found that DHT has a direct effect in suppressing BMSC-to-adipocyte formation. Thus, reducing ADT-induced increases in bone marrow adiposity may be one strategy to prevent or delay PCa relapse in bone. Interestingly, we found that cholesterol biosynthesis pathway was downregulated during DHT-mediated BMSC-to-adipocyte suppression, allowing us to explore inhibition of this pathway for reducing BMSC-to-adipocyte transition. While statins are well-known for its inhibitory effect on HMG-CoA reductase, statins have been shown to reduce adipocyte formation through inhibiting the synthesis of farnesyl pyrophosphate that functions as an endogenous PPARγ agonist [23]. Indeed, we showed that statin treatment can reduce bone marrow adiposity and decrease the proliferation of PCa cells in bone when tumor cells were delivered by

intracardiac injection. Our work suggests that statins may be considered as an approach to prevent or delay PCa relapse in bone before initiation of androgen depletion therapy. Our study is consistent with the clinical observations that statin use in patients undergoing androgen depletion therapy seems to have a beneficial effect in decreasing the incidence of “advanced” or “lethal” PCa [4–6]. Preventing or delaying PCa recurrence in bone will improve the survival of patients with PCa.

Tumor microenvironment (TME) has been shown to play a critical role in tumor progression. Bone marrow TME is especially important as PCa cells preferentially metastasize to bone and metastatic PCa cells in bone are resistant to therapies. That androgen depletion-induced changes in bone marrow adiposity may be involved in the progression of PCa in bone has not been considered. We showed that androgen depletion, the standard treatment for advanced PCa, leads to an increase in bone marrow adiposity that plays a role in enhancing PCa progression in bone. Bone marrow adipocytes develop from a unique progenitor when compared to white adipocytes [29, 30]. Their phenotypes resemble both brown and white adipose tissue [29]. Bone marrow adipocytes have been shown to exhibit endocrine-like functions and release cytokines such as IL-6, IL-1β, TNF-α, leptin, and adipsin, some of which have been shown to affect proliferation, apoptosis and migration of cancer cells [31–34]. Our studies showed that ADT-induced BMSC-to-adipocyte transition increases leptin that enhances PCa cell entry into mitosis and increases cell proliferation. In addition to protein factors, it is possible that increases in bone marrow adiposity has an effect on the metabolic reprogramming of metastatic PCa cells in bone and that may also promote PCa growth in bone [12, 28, 33, 35].

We showed that BMSC transition to adipocytes in castrated mice is directly mediated by AR in bone marrow stromal cells. In human bone/bone marrow, AR has been shown to express in many cell types, including bone marrow stromal cells [36, 37]. These AR-positive cells in the bone marrow stroma are also targets for androgen depletion therapy for prostate cancer. Interestingly, Crnalic et al. [38] showed that in bone metastasis specimens, only few AR-positive cells were found in the metastasis microenvironment. How the invading tumor cells affect the AR status of the stromal cells in the bone marrow is unknown. Whether these observations imply that castration or ADT-induced increase in bone marrow adiposity may be more apparent in patients with non-bone metastatic prostate cancer, as compared to bone metastatic prostate cancer, is also unknown.

We observed that androgens (Fig. 4B) or statins (Fig. 5D) reduce the secretion of leptin during BMSC-to-adipocyte transition. The mechanism, by which androgens or statins repress leptin transcription, is unknown. One possibility is that liganded androgen receptor binds to leptin promoter and represses leptin transcription. However, no androgen receptor binding sequence was found in leptin promoter according to the human gene database GeneCards. The other possibility is that androgen-mediated downregulation of leptin expression is associated with inhibition of adipocyte formation. According to GeneCards, 353 transcription binding sites are found in leptin promoter, including PPARγ, RXRα, and CEBPα. Zhang et al. [39] identified a 17-bp noncanonical PPARγ/RXRα binding site in leptin promoter that is necessary for the fat-regulated control of reporter expression. In our RNAseq analysis, we identified 463 adipogenesis genes, the expressions of which

are suppressed by androgens (Fig.3C). We found that 44 of these 463 gene products are localized in the nucleus based on Ingenuity Pathway Analysis (Fig. 3C). Among these 44 genes, 14 are categorized as transcription factors (Supplementary Table S1), including *Pparγ* and *Cebpα*. These observations suggest that androgens likely downregulate leptin expression through inhibition of *Pparγ* and *Cebpα* expressions. We also found that statins inhibited the expression of *Pparγ* (Fig. 5C). Together, these observations suggest that both androgens and statins downregulate leptin through inhibition of *Pparγ* expression.

Several mechanisms have been presented for how statins may inhibit PCa proliferation. Statins affect many pathways essential for cancer formation and progression through both cholesterol-mediated and non-cholesterol-mediated mechanisms [7]. We found that statins inhibit BMSC-to-adipocyte transition, prompting us to consider that this effect of statins on bone marrow adiposity may contribute to the decrease of PCa progression in bone after androgen depletion therapy. However, because statin affects multiple biological processes, it is possible that statins may affect other processes in addition to BMSC-to-adipocyte transition to inhibit PCa proliferation and PCa progression in bone. Nevertheless, our studies provide a mechanistic understanding to the clinical observations that statin use decreases the incidence of “advanced” or “lethal” PCa but not the overall risk of PCa [4].

In addition to adipocytes, ADT also increases osteoclasts in bone marrow. Ottewell et al. [40] showed that androgen ablation results in growth of disseminated tumor cells in bone through osteoclast-mediated mechanisms. Increased osteolysis may release factors from bone, e.g. TGFβ1, which has been shown to enhance PCa progression in bone [41]. Recently, Jiao et al. [42] reported that osteoclast-mediated bone resorption releases TGFβ that restrains Th1 lineage development. Thus, controlling ADT-induced changes in bone microenvironment, including adipocytes, osteoclasts and immune cells, will be required to further improve treatment outcomes for bone metastatic PCa.

Castrate-resistant recurrence of PCa frequently occurs in bone. However, strategies to prevent such a lethal event are lacking. Our studies raise the possibility of ADT-induced changes in bone marrow adiposity is one contributing factor for PCa recurrence in bone, and further suggest that statins may be considered as a secondary PCa prevention approach to prevent or delay PCa relapse in bone. Further investigation into the effectiveness of statin use in delaying castrate-resistant PCa relapse in bone is warranted.

Material and Methods

Cell lines, antibodies and reagents

Cell lines: Human PCa C4-2B4 (Robert Sikes, University of Delaware, 2006) [43, 44], C4-2b (Leland Chung, Cedars-Sinai Medical Center, 2004) [45], PC3 (ATCC, 2019), 22RV1 (ATCC, 2015) [46, 47]; primary bone marrow-derived stromal cells (BMSCs) were isolated from femurs and tibias of 6-week-old male CD1 mice (Charles River) and maintained in DMEM containing 10% FBS; M2-10B4 cells (ATCC, 2018), a BMSC-derived line from C57BL/6J×C3H/HeJ F1 mouse [16], were maintained in RPMI-1640 with 10% heat-inactivated FBS. Mouse cells were used between 6 to 20 passages. Cell line identity was verified by Short Tandem Repeat analysis. All cells are mycoplasma free. Antibodies: Stat3

(Cell Signaling). Reagents: androgens DHT, R1881; atorvastatin, rosuvastatin, fluvastatin, lovastatin, mevastatin, simvastatin (Sigma-Aldrich); recombinant mouse leptin; mouse leptin quantikine ELISA kit (R&D).

Adipogenic differentiation of BMSC

Confluent cultures of BMSC were changed into adipocyte differentiation medium (ADM) containing 10% charcoal-stripped serum (CSS) supplemented with insulin (2 μg/mL), dexamethasone (1 μM), and rosiglitazone (2 μM) (Sigma-Aldrich). ADM was changed every third day. CSS was prepared from heat-inactivated Opti-Gold FBS (GenDEPOT). Cells in ADM were treated with androgens or statins as indicated. Adipocytes containing oil droplets were visualized with Oil Red O (ORO) staining and ORO-positive cells were counted. ORO was then extracted with 100% isopropyl alcohol and its OD measured at 510 nm.

RNA sequencing and analysis

Total RNA was prepared using TRIzol (Invitrogen) and RNeasy purification kit (Qiagen). RNA sequencing was conducted by Arraystar Inc. (Rockville, MD). RNA sequencing results were analyzed using QIAGEN Ingenuity Pathway Analysis (IPA). To identify pathways that are affected during adipogenesis with or without DHT, datasets with gene identifiers, corresponding expression fold changes, and p values were uploaded to IPA with default settings to match the gene types and locations contained in the Ingenuity Knowledge Base, followed by core analyses. The canonical pathways involved in upregulated and downregulated genes were sorted based on z-scores provided by the IPA program.

Quantitative Real-time PCR Analysis

cDNA was synthesized from 1 μg of total RNA using TaqMan Reverse Transcription Reagents (Life Technologies). To quantify mRNA expression, real-time RT–PCR was performed with a Multiplex Quantitative PCR System (STRATAGENE, Model Mx3000pTM) using SYBR green (Applied Biosystems, CA, USA) fluorescence signals under the following PCR conditions: 40 cycles of 15-second denaturation at 95°C and 1-minute amplification at 60°C. All reactions were run in duplicates and normalized to a mouse housekeeping gene, Glyceraldehyde-3-phosphate dehydrogenase (Gapd). The oligo sequences of the primers used are shown in Supplementary Table S1. The relative mRNA level for each gene was determined using Gapd as a control. DNA from mouse hind legs was quantified by real-time qPCR using human Alu sequence primers (Supplementary Table S2). The number of tumor cells in bone was calculated based on Alu PCR of serial dilutions of DNA from PCa cells.

Short interfering RNA (siRNA)-mediated knockdown of androgen receptor

Androgen receptors in BMSC and M2-10B4 cells were knocked down using siRNA oligos (Supplementary Table S1) and MISSION siRNA reagents (Sigma-Aldrich) according to the manufacturer’s instructions.

Fluorescent ubiquitination-based cell cycle indicator (FUCCI)

C4-2B4 cells were sequentially transduced with two retroviral vectors, one marking G1 and other S-G2M cell cycle phases. Cells were first transduced with pRetroX-G1-Red G1 reporter containing DNA replication factor 1 (CDT) fused with mCherry and selected with puromycin for 7 days [20]. Cells were subsequently transduced with pRetroX-SG2M reporter containing Geminin fused with Cyan and selected with neomycin plus puromycin for 7 days. CDT-mCherry levels peak in G1 but drop after S as CDT-mCherry is degraded by SCF E3 ubiquitin ligase. Geminin-Cyan levels are high in S-G2M but drop in G1 as Geminin-Cyan is degraded by APC ubiquitin ligase. The dynamic shift of C4-2B4-FUCCI cells from G1 (red) into S-G2M (green) was monitored live at the single cell level in a BioStation (Nikon) [48].

Immunofluorescence

C4-2B4 cells treated as indicated were immunostained with Stat3 antibody. Images were acquired on a Nikon TE2000 widefield microscope system. Stat3 fluorescence per nucleus was quantified using NIS-Elements AR5.21.02 (Nikon) software [48].

Animal studies

All animal procedures were performed according to an approved protocol from MD Anderson's Animal Care and Use Committee, in accordance with the recommendations in the NIH Guide for the Care and Use of Laboratory Animals. For statin treatment, male CD1 mice (Taconic Biosciences) were orally administered with atorvastatin (10 mg/kg/day) or vehicle once a day. After 7-10 days, mice were castrated or sham-operated. Atorvastatin treatment was continued for additional 6 weeks. The hind limbs of mice in groups Control (n=5), Castrated (n=5), and Atorvastatin/Castrated (n=7) were used for micro-CT and bone histomorphometry analyses. To examine statin pre-treatment on PCa progression in bone, 20-week-old SCID mice (Taconic Biosciences) were orally administered with atorvastatin or vehicle for 10 days followed by castration. Two weeks after castration, luciferase-Tomato labeled 22RV1 cells (22RV1/LT) (1×10^6 cells in 50 μL per mouse) were injected intra-cardially [49]. Four weeks after tumor inoculation, hind limbs of the mice without (n=9) or with atorvastatin pretreatment (n=10) were extracted for analyses.

Micro-computed tomographic evaluation (micro-CT)

Femurs were fixed in 10% paraformaldehyde for 48 hours at 4°C and analyzed by micro-CT using Bruker SkyScan 1276 (Bruker, Kontich, Belgium). CT Analyzer (Bruker) software (version 1.17.7.2) was used for data analyses.

Bone histomorphometry

Bone histomorphometry analysis was performed on non-decalcified mouse femurs in our Bone Histomorphometry Core Laboratory. Osteoblast and osteoclast measurements were performed on two separate 5 μm thick Toluidine Blue and TRAP stained sections, respectively, separated by a distance of 50 μm, and the data pooled.

Statistical analysis

All data were collected from three or more independent experiments. Results were expressed as mean ± S.D. Graphpad 8.0 Prism was used to perform statistical analyses. Significance of differences between groups was evaluated by Student's t-test or ANOVA. $p < 0.05$ was considered significant.

Supplementary Material

Refer to Web version on PubMed Central for supplementary material.

Acknowledgements

This work was supported by grants from the NIH (CA174798, P50 CA140388, P30 CA016672), Cancer Prevention and Research Institute of Texas (CPRIT RP150179, RP190252), the Prostate Cancer Foundation, and funds from The University of Texas MD Anderson Moonshot Program.

References

1. Watson PA, Arora VK, Sawyers CL. Emerging mechanisms of resistance to androgen receptor inhibitors in prostate cancer. Nat Rev Cancer2015; 15: 701–711. [PubMed: 26563462]
2. Roodman GD. Mechanisms of bone metastasis. N Engl J Med2004; 350: 1655–1664. [PubMed: 15084698]
3. Logothetis CJ, Gallick GE, Maity SN, Kim J, Aparicio A, Efstathiou Eet al.Molecular classification of prostate cancer progression: foundation for marker-driven treatment of prostate cancer. Cancer discovery2013; 3: 849–861. [PubMed: 23811619]
4. Platz EA, Leitzmann MF, Visvanathan K, Rimm EB, Stampfer MJ, Willett WCet al.Statin drugs and risk of advanced prostate cancer. J Natl Cancer Inst2006; 98: 1819–1825. [PubMed: 17179483]
5. Gordon JA, Buonerba C, Pond G, Crona D, Gillessen S, Lucarelli Get al.Statin use and survival in patients with metastatic castration-resistant prostate cancer treated with abiraterone or enzalutamide after docetaxel failure: the international retrospective observational STABEN study. Oncotarget2018; 9: 19861–19873. [PubMed: 29731989]
6. Harshman LC, Wang X, Nakabayashi M, Xie W, Valenca L, Werner Let al.Statin Use at the Time of Initiation of Androgen Deprivation Therapy and Time to Progression in Patients With Hormone-Sensitive Prostate Cancer. JAMA Oncol2015; 1: 495–504. [PubMed: 26181260]
7. Alfaqih MA, Allott EH, Hamilton RJ, Freeman MR, Freedland SJ. The current evidence on statin use and prostate cancer prevention: are we there yet?Nature reviews Urology2017; 14: 107–119. [PubMed: 27779230]
8. Lee YC, Lin SC, Yu G, Cheng CJ, Liu B, Liu HCet al.Identification of Bone-Derived Factors Conferring De Novo Therapeutic Resistance in Metastatic Prostate Cancer. Cancer Res2015; 75: 4949–4959. [PubMed: 26530902]
9. Logothetis C, Lin S-H. Osteoblasts in prostate cancer metastasis to bone. Nature Reviews Cancer2005; 5: 21–28. [PubMed: 15630412]
10. Calvi LM, Link DC. The hematopoietic stem cell niche in homeostasis and disease. Blood2015; 126: 2443–2451. [PubMed: 26468230]
11. Diedrich J, Gusky HC, Podgorski I. Adipose tissue dysfunction and its effects on tumor metabolism. Horm Mol Biol Clin Investig2015; 21: 17–41.
12. Herroon MK, Rajagurubandara E, Hardaway AL, Powell K, Turchick A, Feldmann Det al.Bone marrow adipocytes promote tumor growth in bone via FABP4-dependent mechanisms. Oncotarget2013; 4: 2108–2123. [PubMed: 24240026]
13. Sharifi N, Gulley JL, Dahut WL. An update on androgen deprivation therapy for prostate cancer. Endocrine-related cancer2010; 17: R305–315. [PubMed: 20861285]

14. Gimble JM, Robinson CE, Wu X, Kelly KA. The function of adipocytes in the bone marrow stroma: an update. Bone1996; 19: 421–428. [PubMed: 8922639]
15. Tencerova M, Kassem M. The Bone Marrow-Derived Stromal Cells: Commitment and Regulation of Adipogenesis. Front Endocrinol (Lausanne)2016; 7: 127. [PubMed: 27708616]
16. Sutherland HJ, Eaves CJ, Lansdorp PM, Thacker JD, Hogge DE. Differential regulation of primitive human hematopoietic cells in long-term cultures maintained on genetically engineered murine stromal cells. Blood1991; 78: 666–672. [PubMed: 1713512]
17. Lucas-Herald AK, Alves-Lopes R, Montezano AC, Ahmed SF, Touyz RM. Genomic and non-genomic effects of androgens in the cardiovascular system: clinical implications. Clin Sci (Lond)2017; 131: 1405–1418. [PubMed: 28645930]
18. Lin D, Alberton P, Caceres MD, Volkmer E, Schieker M, Docheva D. Tenomodulin is essential for prevention of adipocyte accumulation and fibrovascular scar formation during early tendon healing. Cell Death Dis2017; 8: e3116. [PubMed: 29022912]
19. Sato K, Emi M, Ezura Y, Fujita Y, Takada D, Ishigami Tet al.Soluble epoxide hydrolase variant (Glu287Arg) modifies plasma total cholesterol and triglyceride phenotype in familial hypercholesterolemia: intrafamilial association study in an eight-generation hyperlipidemic kindred. J Hum Genet2004; 49: 29–34. [PubMed: 14673705]
20. Sakaue-Sawano A, Kurokawa H, Morimura T, Hanyu A, Hama H, Osawa Het al.Visualizing spatiotemporal dynamics of multicellular cell-cycle progression. Cell2008; 132: 487–498. [PubMed: 18267078]
21. Saxena NK, Vertino PM, Anania FA, Sharma D. leptin-induced growth stimulation of breast cancer cells involves recruitment of histone acetyltransferases and mediator complex to CYCLIN D1 promoter via activation of Stat3. J Biol Chem2007; 282: 13316–13325. [PubMed: 17344214]
22. Azemawah V, Movahed MR, Centuori P, Penaflor R, Riel PL, Situ Set al.State of the Art Comprehensive Review of Individual Statins, Their Differences, Pharmacology, and Clinical Implications. Cardiovasc Drugs Ther2019; 33: 625–639. [PubMed: 31773344]
23. Goto T, Nagai H, Egawa K, Kim YI, Kato S, Taimatsu Aet al.Farnesyl pyrophosphate regulates adipocyte functions as an endogenous PPARgamma agonist. Biochem J2011; 438: 111–119. [PubMed: 21605082]
24. Xu L, Shen M, Chen X, Zhu R, Yang DR, Tsai Yet al.Adipocytes affect castration-resistant prostate cancer cells to develop the resistance to cytotoxic action of NK cells with alterations of PD-L1/NKG2D ligand levels in tumor cells. Prostate2018; 78: 353–364. [PubMed: 29330929]
25. Laurent V, Guerard A, Mazerolles C, Le Gonidec S, Toulet A, Nieto Let al.Periprostatic adipocytes act as a driving force for prostate cancer progression in obesity. Nat Commun2016; 7: 10230. [PubMed: 26756352]
26. Laurent V, Toulet A, Attane C, Milhas D, Dauvillier S, Zaidi Fet al.Periprostatic Adipose Tissue Favors Prostate Cancer Cell Invasion in an Obesity-Dependent Manner: Role of Oxidative Stress. Molecular cancer research : MCR2019; 17: 821–835. [PubMed: 30606769]
27. Tang KD, Liu J, Jovanovic L, An J, Hill MM, Vela Iet al.Adipocytes promote prostate cancer stem cell self-renewal through amplification of the cholecystokinin autocrine loop. Oncotarget2016; 7: 4939–4948. [PubMed: 26700819]
28. Diedrich JD, Rajagurubandara E, Herroon MK, Mahapatra G, Huttemann M, Podgorski I. Bone marrow adipocytes promote the Warburg phenotype in metastatic prostate tumors via HIF-1alpha activation. Oncotarget2016; 7: 64854–64877. [PubMed: 27588494]
29. Tavassoli MMarrow adipose cells. Ultrastructural and histochemical characterization. Archives of pathology1974; 98: 189–192. [PubMed: 4137056]
30. Tavassoli MUltrastructural development of bone marrow adipose cell. Acta Anat (Basel)1976; 94: 65–77. [PubMed: 961340]
31. Caers J, Deleu S, Belaid Z, De Raeve H, Van Valckenborgh E, De Bruyne Eet al.Neighboring adipocytes participate in the bone marrow microenvironment of multiple myeloma cells. Leukemia2007; 21: 1580–1584. [PubMed: 17377589]
32. Liu Z, Xu J, He J, Liu H, Lin P, Wan Xet al.Mature adipocytes in bone marrow protect myeloma cells against chemotherapy through autophagy activation. Oncotarget2015; 6: 34329–34341. [PubMed: 26455377]

33. Hardaway AL, Herroon MK, Rajagurubandara E, Podgorski I. Bone marrow fat: linking adipocyte-induced inflammation with skeletal metastases. Cancer Metastasis Rev2014; 33: 527–543. [PubMed: 24398857]
34. Morris EV, Edwards CM. Adipokines, adiposity, and bone marrow adipocytes: Dangerous accomplices in multiple myeloma. J Cell Physiol2018; 233: 9159–9166. [PubMed: 29943829]
35. Hardaway AL, Herroon MK, Rajagurubandara E, Podgorski I. Marrow adipocyte-derived CXCL1 and CXCL2 contribute to osteolysis in metastatic prostate cancer. Clin Exp Metastasis2015; 32: 353–368. [PubMed: 25802102]
36. Abu EO, Horner A, Kusec V, Triffitt JT, Compston JE. The localization of androgen receptors in human bone. The Journal of clinical endocrinology and metabolism1997; 82: 3493–3497. [PubMed: 9329391]
37. Mantalaris A, Panoskaltsis N, Sakai Y, Bourne P, Chang C, Messing EMet al.Localization of androgen receptor expression in human bone marrow. J Pathol2001; 193: 361–366. [PubMed: 11241417]
38. Crnalic S, Hornberg E, Wikstrom P, Lerner UH, Tieva A, Svensson Oet al.Nuclear androgen receptor staining in bone metastases is related to a poor outcome in prostate cancer patients. Endocrine-related cancer2010; 17: 885–895. [PubMed: 20688881]
39. Zhang Y, Dallner OS, Nakadai T, Fayzikhodjaeva G, Lu YH, Lazar MAet al.A noncanonical PPARgamma/RXRalpha-binding sequence regulates leptin expression in response to changes in adipose tissue mass. Proc Natl Acad Sci U S A2018; 115: E6039–E6047. [PubMed: 29891714]
40. Ottewell PD, Wang N, Meek J, Fowles CA, Croucher PI, Eaton CLet al.Castration-induced bone loss triggers growth of disseminated prostate cancer cells in bone. Endocrine-related cancer2014; 21: 769–781. [PubMed: 25052474]
41. Sato S, Futakuchi M, Ogawa K, Asamoto M, Nakao K, Asai Ket al.Transforming growth factor beta derived from bone matrix promotes cell proliferation of prostate cancer and osteoclast activation-associated osteolysis in the bone microenvironment. Cancer science2008; 99: 316–323. [PubMed: 18271931]
42. Jiao S, Subudhi SK, Aparicio A, Ge Z, Guan B, Miura Yet al.Differences in Tumor Microenvironment Dictate T Helper Lineage Polarization and Response to Immune Checkpoint Therapy. Cell2019; 179: 1177–1190 e1113. [PubMed: 31730856]
43. Wu TT, Sikes RA, Cui Q, Thalmann GN, Kao C, Murphy CFet al.Establishing human prostate cancer cell xenografts in bone: induction of osteoblastic reaction by prostate-specific antigen-producing tumors in athymic and SCID/bg mice using LNCaP and lineage-derived metastatic sublines. Int J Cancer1998; 77: 887–894. [PubMed: 9714059]
44. Thalmann GN, Sikes RA, Wu TT, Degeorges A, Chang SM, Ozen Met al.LNCaP progression model of human prostate cancer: androgen-independence and osseous metastasis. Prostate2000; 44: 91–103. [PubMed: 10881018]
45. Thalmann GN, Anezinis PE, Chang S, Zhau HE, Kim E, Hopwood VLet al.Androgen-independent cancer progression and bone metastasis in the LNCaP model of human prostate cancer. Cancer Res1994; 54: 2577–2581. [PubMed: 8168083]
46. Wainstein MA, He F, Robinson D, Kung HJ, Schwartz S, Giaconia JMet al.CWR22: androgen-dependent xenograft model derived from a primary human prostatic carcinoma. Cancer Res1994; 54: 6049–6052. [PubMed: 7525052]
47. Sramkoski RM, Pretlow TG 2nd, Giaconia JM, Pretlow TP, Schwartz S, Sy MSet al.A new human prostate carcinoma cell line, 22Rv1. In Vitro Cell Dev Biol Anim1999; 35: 403–409. [PubMed: 10462204]
48. Yu-Lee LY, Yu G, Lee YC, Lin SC, Pan J, Pan Tet al.Osteoblast-Secreted Factors Mediate Dormancy of Metastatic Prostate Cancer in the Bone via Activation of the TGFbetaRIII-p38MAPK-pS249/T252RB Pathway. Cancer Res2018; 78: 2911–2924. [PubMed: 29514796]
49. Lee YC, Jin JK, Cheng CJ, Huang CF, Song JH, Huang Met al.Targeting constitutively activated beta1 integrins inhibits prostate cancer metastasis. Molecular cancer research : MCR2013; 11: 405–417. [PubMed: 23339185]

Significance

This study provides mechanistic insights into how statins suppress BMSC-to-adipocyte transition in the tumor microenvironment and offers a rationale for developing statins as a secondary prevention to delay PCa relapse in bone.

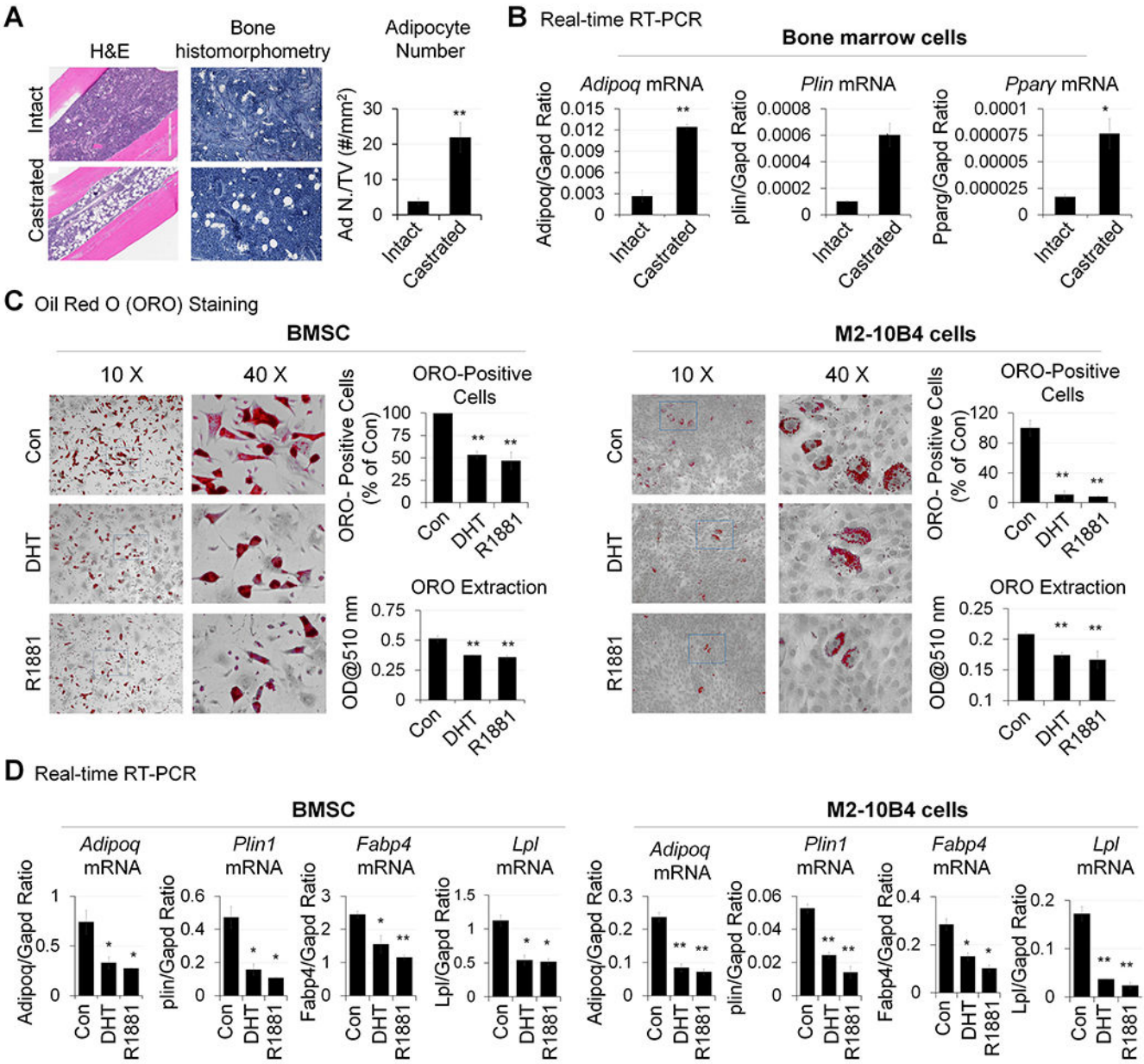

Fig. 1. Castration enhances while androgens suppress BMSC-to-adipocyte transition.

(A) H&E of femur in intact and castrated mice (left). Bone histomorphometry analyses (Toluidine blue staining) of adipocytes in the femur of intact and castrated mice (middle). Number of adipocytes per area was measured based on bone histomorphometry (right). (B) Bone marrow cells from femurs of intact and castrated mice were analyzed by qRT-PCR for adipocyte markers adiponectin (*Adipoq*), perilipin 1 (*Plin1*) and *PPARγ*. (C) Bone marrow stromal cells (BMSC) and bone marrow stromal cell line M2-10B4 were cultured in adipocyte differentiation medium (ADM), in the presence or absence of androgens DHT or R1881 (10 nM each) for 5 days. Adipocyte formation was determined by Oil red-O (ORO) staining, counting ORO-positive cells in 10 – 15 fields each, and quantification of ORO after

extraction from 3 – 4 independent experiments. (D) qRT-PCR for adipocyte-related gene expression in cells treated in C. *p <0.05; **p <0.01.

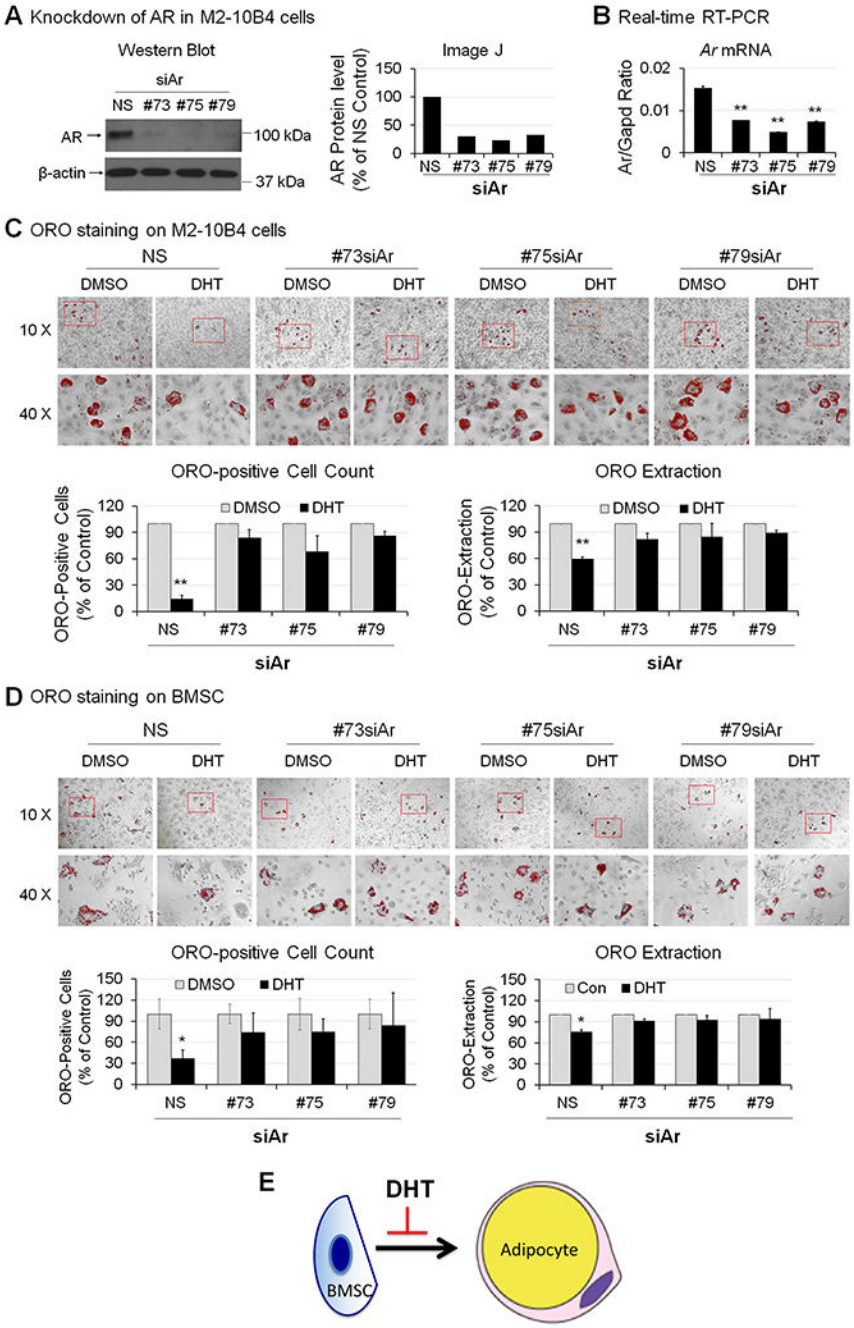

Fig. 2. Androgen receptor mediates suppression of BMSC-to-adipocyte transition by DHT.

Transient knockdown of androgen receptor (AR) by siRNA in M2-10B4 cells was verified by (A) western blot and (B) qRT-PCR. (C) Oil red-O (ORO) staining and quantification in M2-10B4-#73si*Ar*, M2-10B4-#75si*Ar* and M2-10B4-#79si*Ar* clones and M2-10B4-NS (non-silencing) control following ADM with or without DHT. (D) AR was knocked down in BMSC as in A and analyzed as in C. *p <0.05; **p <0.01. (E) Illustration depicting that DHT directly suppresses BMSC-to-adipocyte transition.

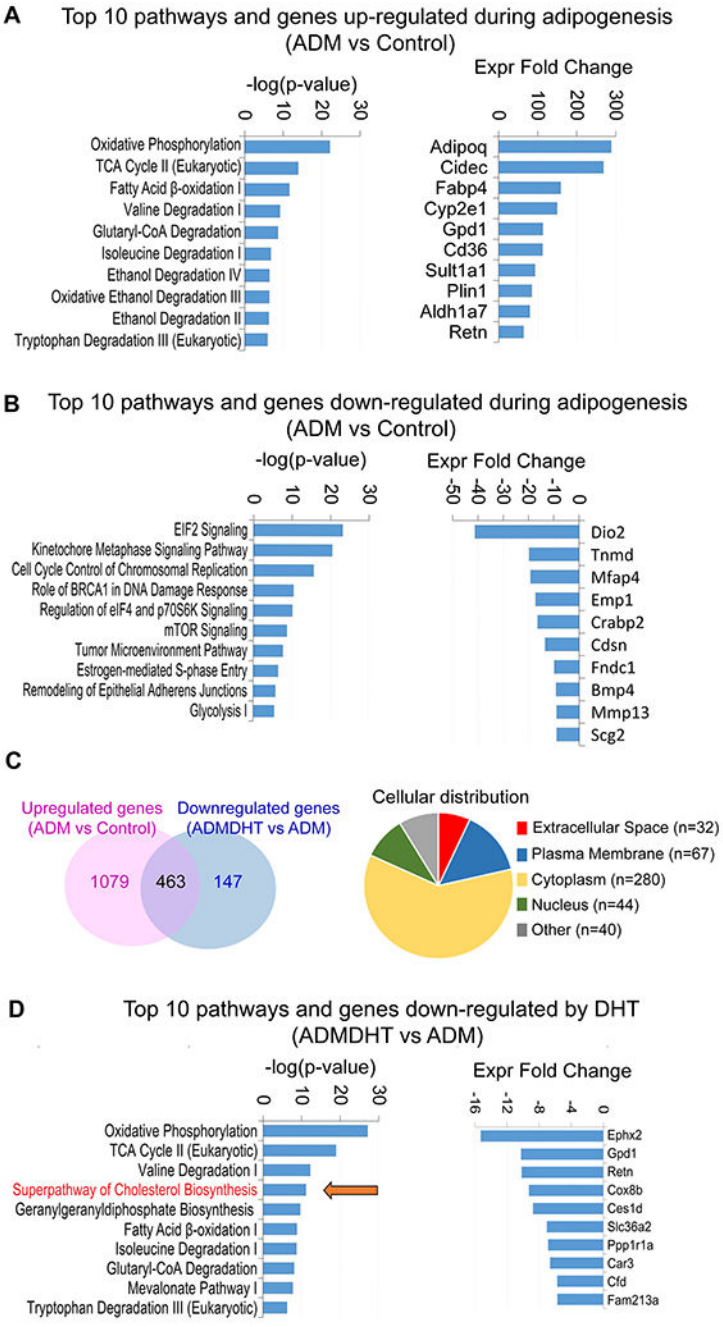

Fig. 3. RNAseq analysis of changes in gene expression during BMSC-to-adipocyte transition with or without DHT treatment.

RNAs prepared from M2-10B4 cells cultured with or without ADM and treated with or without DHT were subjected to RNAseq analysis. (A) Pathways and gene transcripts up-regulated during adipogenesis (ADM vs control). (B) Pathways and gene transcripts down-regulated during adipogenesis (ADM vs control). (C) Venn diagram of genes up-regulated during adipogenesis and genes down-regulated by DHT treatment during adipogenesis (left). Cellular distribution of commonly regulated genes (right). (D) Pathways and gene transcripts down-regulated by DHT during BMSC-to-adipocyte transition (ADMDHT vs ADM).

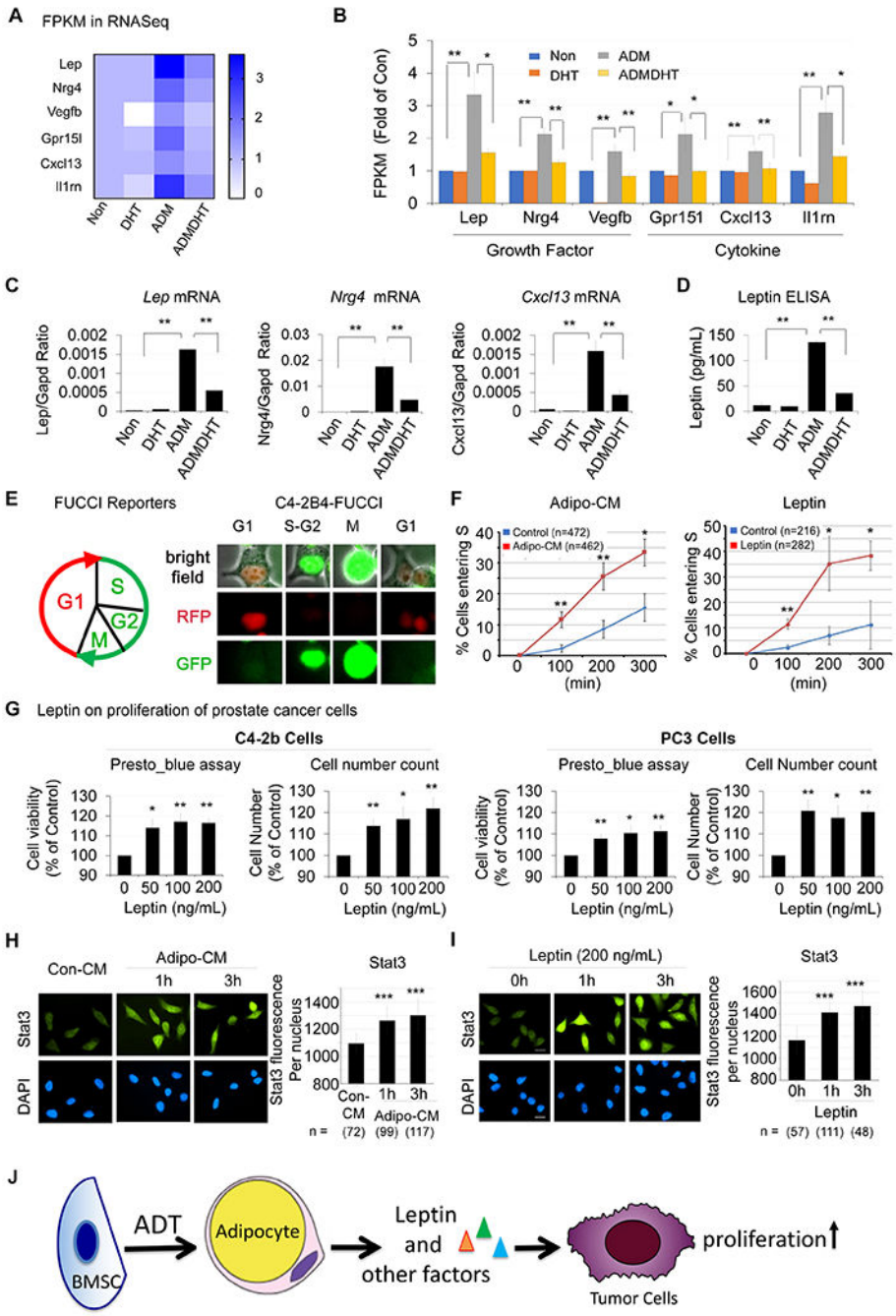

Fig. 4. Adipocyte-conditioned medium and leptin stimulate prostate cancer cell cycle progression and cell proliferation.

(A) Heatmap and (B) expression (fold over control) of DHT-regulated growth factors and cytokines in M2-10B4 cells treated as indicated. (C) qRT-PCR for mRNA of three secreted factors in cells treated as indicated. (D) ELISA of leptin protein levels in the conditioned media (CM) of cells treated as indicated. (E) Fluorescent ubiquitination-based cell cycle indicator (FUCCI) system containing two fluorescent reporters that label G1 phase nuclei red and S-G2M phase nuclei green (left). Live cell imaging following a single C4-2B4-FUCCI cell through G1 (red) into S-G2M (green) and back to G1 (red) after cell

division (right). (F) % cells entering S phase when C4-2B4-FUCCI cells were incubated with Adipo-CM or control CM, or with or without 100 ng/mL leptin. n, number of cells analyzed in N independent experiments: CM (N=5 each), leptin (N=3) or control (N=2). (G) Leptin stimulates C4-2b and PC-3 cell proliferation, as measured by Presto blue assays and cell counting. C4-2B4 cells were treated with either Adipo-CM (H) or leptin (I) as indicated and immunostained with Stat3 antibody. Nuclear Stat3 fluorescence signals were quantified by NIS-Elements. n, number of nuclei analyzed. Bars, 20 μm. *p <0.05, **p <0.01, ***p <0.001. (J) Summary. ADT enhances BMSC-to-adipocyte transition, leading to an increase in adipocyte-secreted factors, some of which stimulate PCa cell proliferation.

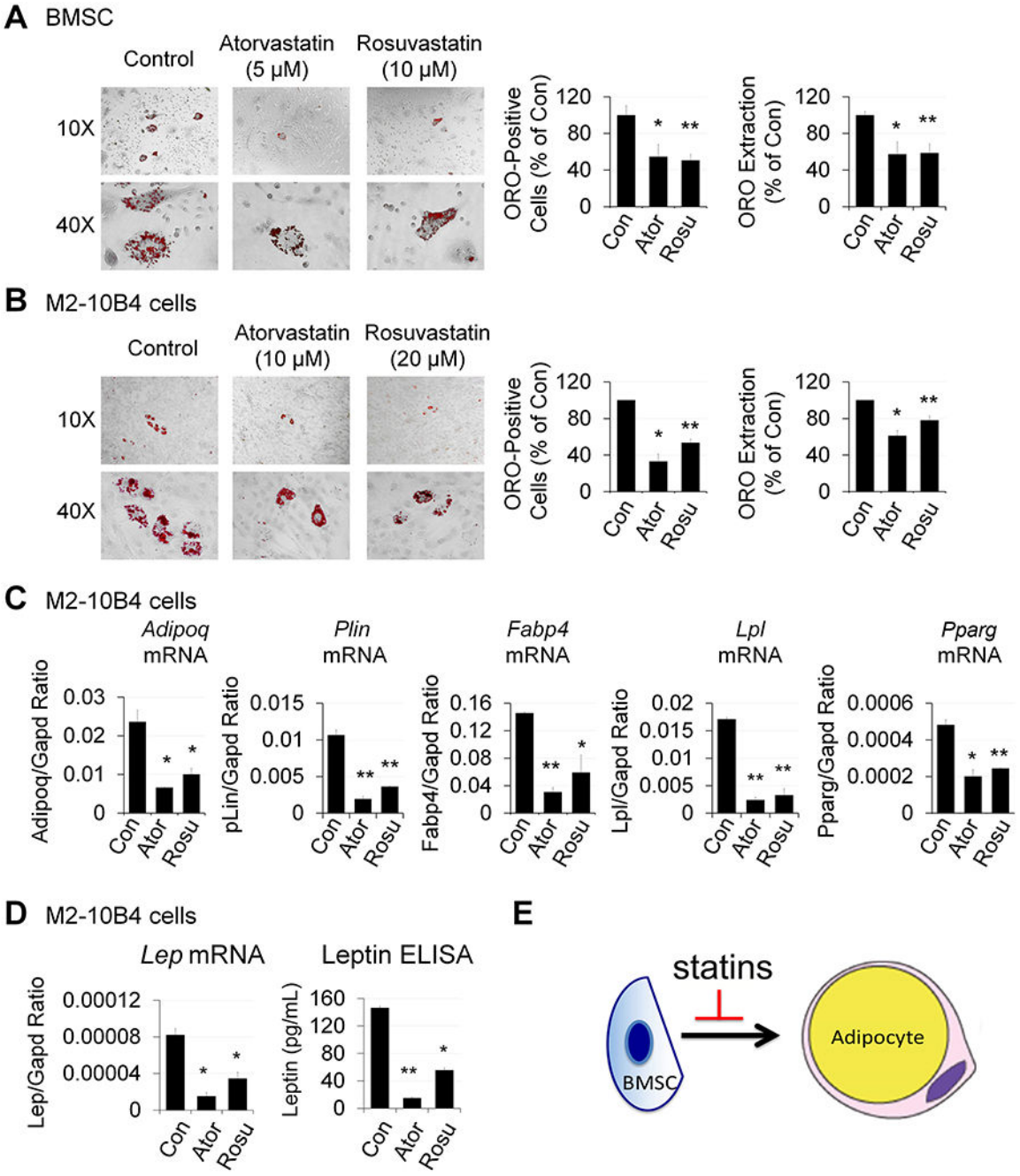

Fig. 5. Statins inhibit BMSC-to-adipocyte transition *in vitro*.

Treatment of (A) BMSC or (B) M2-10B4 cells with atorvastatin or rosuvastatin during adipogenesis (ADM) followed with ORO staining, cell counting and ORO quantification. (C) qRT-PCR for adipocyte markers in M2-10B4 cells treated as in B. (D) Leptin RNA (qRT-PCR) and protein (ELISA) levels in cells treated as in B. *p <0.05, **p <0.01. (E) Illustration depicting that statins inhibit BMSC-to-adipocyte transition.

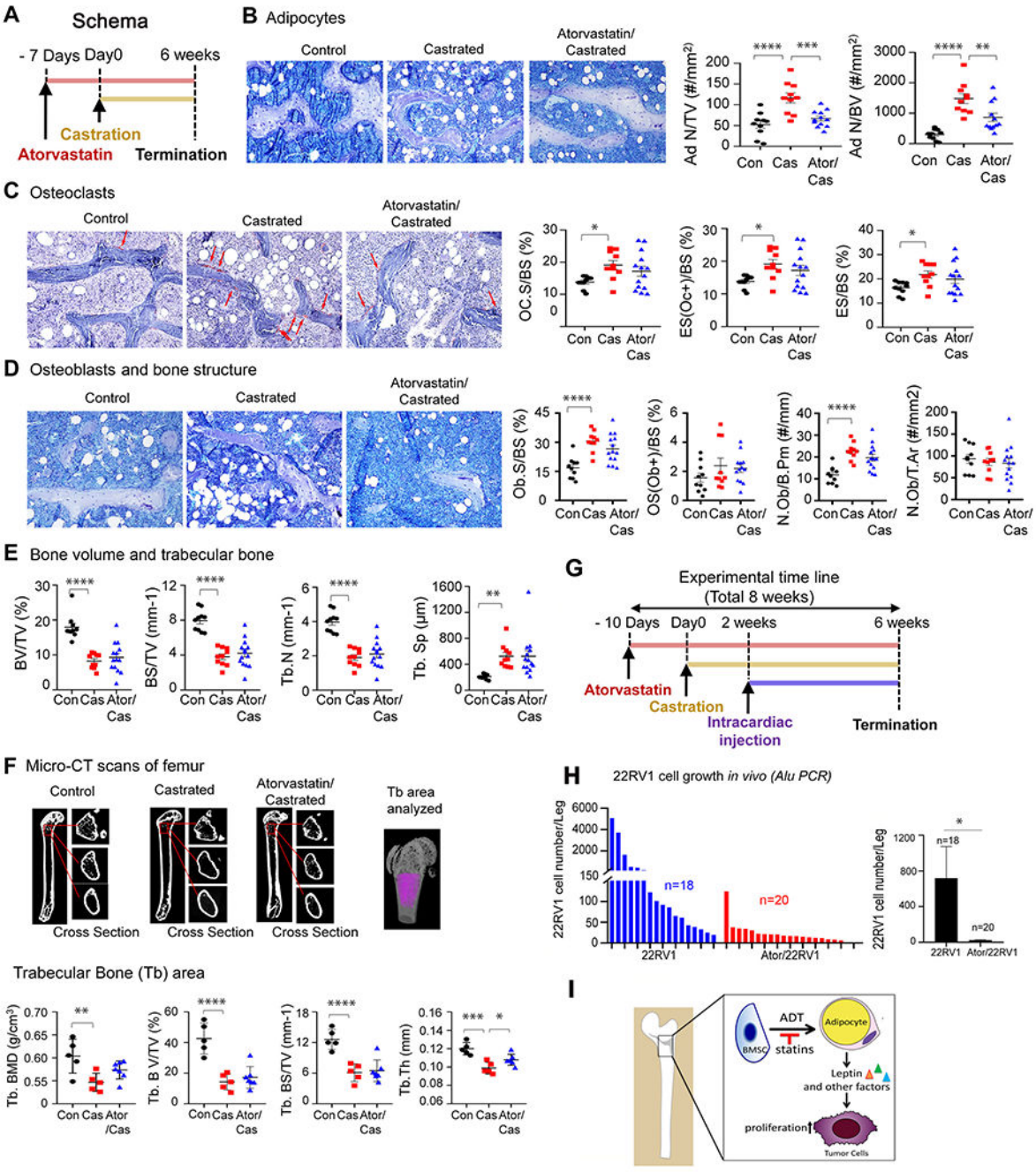

Fig. 6. Statins suppress BMSC-to-adipocyte transition and reduce prostate cancer progression in bone *in vivo*.

(A) Atorvastatin treatment in castrated CD1 mice. (B-E) Bone histomorphometry analysis of (B) adipocytes, (C) osteoclasts (red arrows), (D) osteoblasts, (E) bone volume and trabecular bone. (F) Micro-CT analysis of trabecular bone. Upper, high-resolution scans of femur and cross sections of trabecular bone. Lower, analysis of trabecular bone area. (G) SCID mice with or without atorvastatin oral administration were castrated and 22RV1/LT cells inoculated by intracardiac injection as indicated. (H) Left, number of 22RV1 cells per individual femur was determined by qPCR using primers specific for human *Alu*

repetitive sequence. Right, average number of tumor cells in femurs of mice with or without atorvastatin treatment. n, number of mice per group. *p <0.05, **p <0.01, ***p <0.001, ****p <0.0001. (I) Summary. Androgen depletion enhances BMSC-to-adipocyte transition, leading to increased secretion of adipocyte factors, which stimulate PCa cell proliferation and PCa progression in bone. Statins suppress BMSC-to-adipocyte transition, lower the levels of adipocyte-secreted factors and reduce PCa progression in bone.